NASA CONTRACTOR REPORT 191467

# *FATIGUE-LIFE BEHAVIOR AND MATRIX FATIGUE CRACK SPACING IN UNNOTCHED SCS-6/Timetal® 21S METAL MATRIX COMPOSITES*

**G. T. Ward, D. J. Herrmann, and B. M. Hillberry**
**Purdue University**
**West Lafayette, IN**

**Grant NAGI-1316**

**JULY 1993**



**National Aeronautics and Space Administration**

**LANGLEY RESEARCH CENTER**
**Hampton, Virginia 23681-0001**

# FATIGUE-LIFE BEHAVIOR AND MATRIX FATIGUE CRACK SPACING IN UNNOTCHED SCS-6/Timetal®21S METAL MATRIX COMPOSITES

by

G. T. Ward*, D. J. Herrmann*, and B. M. Hillberry**
School of Mechanical Engineering
Purdue University
West Lafayette, IN 47907

Fatigue tests of the SCS-6/Timetal®21S composite system were performed to characterize the fatigue behavior for unnotched conditions. The stress-life behavior of the unnotched $[0/90]_{2S}$ laminates was investigated for stress ratios of R = 0.1 and R = 0.3. The occurrence of matrix cracking was also examined in these specimens. This revealed multiple matrix crack initiation sites throughout the composite, as well as evenly spaced surface cracks along the length of the specimens. No difference in fatigue lives were observed for stress ratios of R = 0.1 and R = 0.3 when compared on a stress range basis. The unnotched SCS-6/Timetal®21S composites had shorter fatigue lives than the SCS-6/Ti-15-3 composites, however the neat Timetal®21S matrix material had a longer fatigue life than the neat Ti-15-3.

KEY WORDS: Fatigue, titanium matrix, silicon-carbide fibers, unnotched, cross-ply laminates, matrix fatigue crack spacing

---

* Graduate Research Assistant

** Professor

# INTRODUCTION

As aerospace technology reaches toward flying at hypersonic speeds, the research and development of metal matrix composites is becoming increasingly important. When traveling at such speeds, the vehicle will undergo very high thermal as well as mechanical stresses. This requires the skin of the vehicle to have high strength and toughness over a wide temperature range, and to reach such speeds, it must be low in weight. Titanium matrix composites are currently being investigated as possible materials to serve such purposes, due to their light weight, as well as their high temperature properties.

Before the behavior of any material at elevated temperatures can be completely understood, the material must first be investigated at room temperature. The research presented in this report examines the room temperature fatigue behavior of a titanium (Timetal®21S) matrix reinforced with silicon carbide (SCS-6) fibers. Considerable work has recently been done in investigating a similar titanium (Ti-15-3) matrix composite reinforced with the same SCS-6 fibers. Johnson et al. [1] characterized the fatigue properties of unnotched SCS-6/Ti-15-3 composites at room temperature. Many of the procedures that they used were duplicated in the present work on SCS-6/Timetal®21S as a basis for comparison between the two material systems.

Because much of the fatigue damage initiation and propagation in a composite material occurs in the matrix, it is necessary to characterize the fatigue properties of the matrix alone before trying to comprehend the fatigue results of the composite. Therefore, several fatigue tests were performed on "fiberless" Timetal®21S specimens to establish the strain-life behavior of the matrix material.

Room temperature fatigue behavior of unnotched SCS-6/Timetal®21S with cross-ply fiber orientation was investigated. Tests were run at two different stress ratios and the results compared with SCS-6/Ti-15-3 results. Optical and scanning electron microscopy (SEM) were used to determine the damage and failure mechanisms controlling the behavior of these materials.

## MATERIALS AND METHODS

### Materials

The material studied in this research was the SCS-6/Timetal®21S titanium matrix composite. The name Timetal®21S (previously called Ti-β21S) is a shorthand specification for Ti-15Mo-3Al-2.7Nb-0.2Si, which is a metastable beta titanium alloy. The titanium matrix was reinforced with continuous silicon-carbide ceramic fibers, which are used to improve the mechanical properties of the composite in the fiber direction. The 0.14mm diameter fibers, designated as SCS-6,[1] are comprised of silicon around a carbon core.

The composite laminates were fabricated with no weave material by hot-pressing SCS-6 fiber tapes sandwiched between Timetal®21S foils at 1000°C. The plates were then cooled to 621°C and aged for eight hours to relieve any residual stresses, and finally cooled to room temperature. Neat Timetal®21S material was made by the same process as the laminate but without the SCS-6 fibers. Textron[1] manufactured all materials used in this study. Fiber and matrix material properties are given in Table 1. The fibers were assumed to be isotropic.

### Test Specimens

Two different specimen geometries were used in this research. For the neat matrix material, "dogbone" shape specimens with a 51mm gage length and 18mm gage width were used. A fillet radius of 25.4mm was used to minimize the stress concentration while maximizing grip area. The specimens had a mean as-received thickness of 1.0mm. Flat specimens with no reduced gage section were used for the unnotched fatigue tests of the SCS-6/Timetal®21S $[0/90]_{2S}$ composite laminates. These specimens were cut from two different laminated plates with slightly different volume fractions, 0.365 and 0.354. These specimens had a nominal width of 13mm and a mean thickness of 1.75mm. The two specimen geometries are shown in Figure 1. All specimens were cut using a diamond wheel saw.

### Mechanical Testing

Mechanical testing was performed using a 44.5kN (10,000 pound) closed-loop, servo-hydraulic test system, controlled with a software program developed for a Sun 3 workstation [2]. Strains were measured using an extensometer with a gage length of 10.0mm that measures strains up to a maximum of 0.15mm/mm. The knife edges of the extensometer were held in place on the

---

[1]Textron Specialty Material Division, Lowell, Massachusetts

edge of the reduced gage section using small dots of a quick-drying epoxy bonding agent and orthodontic rubber bands around the specimen. Surfaloy[2] coated wedges were used in the hydraulic grips.

*Neat Matrix Fatigue Tests*

The dogbone shaped neat Timetal®21S specimens were cycled in strain-control using the extensometer in the control loop. The tests were run at 10.0Hz, however, the first 40 cycles were run at 2.0Hz and the next 60 cycles at 5.0Hz so that the automatic feedback system used in the controlling program could be used more efficiently. The strain-controlled tests were run with a strain ratio of R = 0.1. A test matrix was developed in an attempt to achieve an even distribution of fatigue lives as well as provide a good estimate of the endurance limit for the matrix material. Failure was taken to be final fracture of the specimen.

*Unnotched Composite Fatigue Tests*

Fatigue tests of unnotched $[0/90]_{2S}$ laminates were run in stress-control. Strain was measured with the extensometer, which was mounted to the specimens in the same manner as described earlier. The tests were divided into two sets, corresponding to the plates from which the specimens were cut. The specimens with a fiber volume fraction of $V_f = 0.365$ were tested at R = 0.1, and those with $V_f = 0.354$ were tested at R = 0.3. Final specimen fracture was also used as the failure criterion for these tests. The test matrix for this group of tests was developed from results of the SCS-6/Ti-15-3 composite [1] to maintain consistent comparisons of the two composite systems.

Objectives for these tests, other than characterizing room temperature stress-life behavior, included investigating fiber/matrix interface debonding in 90° plies and matrix cracking. To check for failure of the 90 degree fiber/matrix interface, edge replicas were taken prior to cycling and at the maximum load of the first cycle. Johnson et al. [1] have shown that for the SCS-6/Ti-15-3 composite, fiber/matrix interface debonding occurs in the 90 degree ply during the first cycle when the thermal residual stress and bond strength are overcome. This can be observed as a knee in the stress-strain curve. For the purpose of checking for this debonding, the first five cycles were run in a quasi-static fashion with low-frequency triangle waves, during which the first cycle was held at maximum load to make the edge replica. The next blocks of 35 and 60 cycles were run at 2.0 and 5.0Hz, respectively, for consistency with the neat matrix material. The remainder of the tests

[2]Registered trademark of MTS Systems Corp.

were conducted at 10.0Hz. Surface and edge replicas were taken periodically to examine matrix cracking. To eliminate any contamination or etching of the titanium due to acetone impurities, the highest available grade was used for making the replicas. Final fracture surfaces were examined with a scanning electron microscope (SEM) to view matrix cracking, ductile fracture, fiber pull-out, as well as other phenomena.

Fatigue Crack Spacing Predictions

The understanding of matrix cracking in metal matrix composites is important, because the matrix is designed to carry a large portion of the load. The existence of matrix cracking will reduce the amount of load the matrix can carry, thus decreasing the composite stiffness and strength. The extent of this stiffness and strength reduction is a function of the density of the matrix cracks.

The potential for a crack to form depends on the stress level in the material. In the case where a matrix crack exists in the composite, the matrix stress is zero at the crack surface. Load is transferred back to the matrix as the distance from the crack increases along the fiber. At a certain distance, the stress in the matrix becomes sufficient to form another crack. To predict this crack spacing, it is necessary to understand the fiber/matrix load transfer near a matrix crack.

Several models have been developed to calculate the load transfer between the fiber and the matrix due to a crack in either component. One common approach within these models is the concentric cylinder model with the inner cylinder representing the fiber and the outer cylinder representing the matrix. Three different models that use this concept are presented in the next sections. Each model can be used to calculate the spacing between uniform cracks, as well as the resulting loss in composite stiffness.

*Cox Shear-Lag Model Applied to Matrix Crack*

Cox [3] developed a model in 1952 to describe the elastic behavior and strength of paper and other fibrous materials. The fibers in this model were considered to be discontinuous, so the model was used for the ends of fibers terminating in the matrix. This approach may also be applied to continuous fibers that have cracked [4]. Hillberry and Johnson [5] derived a similar model relevant for a composite that contains a crack in the matrix, assuming the fiber/matrix interface is fully bonded. This model calculates load transfer by using the shear-lag assumption that fiber/matrix load transfer along the interface is directly proportional to the relative displacement between the fiber and the matrix. For a crack in the matrix,

$$\frac{dP_m}{dx} = H(u - v) \tag{1}$$

where $P_m$ = load in matrix
$x$ = distance from crack along fiber
$H$ = constant to be determined
$u$ = matrix displacement
$v$ = fiber displacement

In addition to the basic shear lag assumption, this model also assumes that the load is transferred from the matrix to the rest of the composite material. The results derived by Hillberry and Johnson [5] show that the matrix stress along the length of the fiber can be written as

$$\sigma_m = E_m \varepsilon \left[ 1 - \frac{\cosh[\beta(L - x)]}{\cosh(\beta L)} \right] \tag{2}$$

where $\beta = \frac{1}{r_f} \left[ \frac{-2V_f}{(1 + \nu_m)(1 - V_f)\ln(V_f)} \right]^{1/2}$
$\sigma_m$ = matrix stress along fiber
$E_m$ = elastic modulus of matrix
$\varepsilon$ = composite strain
$V_f$ = fiber volume fraction
$\nu_m$ = Poisson ratio of matrix
$2L$ = crack spacing

The crack spacing, 2L, can then be calculated using equation (2), where L approaches infinity for 100 percent load transfer. Hillberry and Johnson [5] used the criterion that a crack may form when the matrix stress reaches 95 percent of the maximum stress, resulting in finite crack spacing predictions. Therefore, L is independent of the applied stress level under fully bonded conditions, and can be calculated as

$$L = \frac{1}{\beta} \cosh^{-1} \left( 1 - \frac{\sigma_m(L)}{\sigma_m^{\infty}} \right)^{-1} \tag{3}$$

where $$\frac{\sigma_m(L)}{\sigma_m^{\infty}} = \frac{\sigma_m(L)}{E_m\varepsilon} = 0.95$$

Due to symmetry, two cracks existing in the matrix material must have a minimum distance between them of 2L.

*ACK Shear-Lag Model*

Aveston and Kelly [6] developed a concentric cylinder shear-lag model for full fiber/matrix bonding based on a previous model [7] for the case of a completely debonded fiber/matrix interface. In this model, all of the load from the matrix is transferred to the fiber at the crack tip, rather than to the remainder of the composite. Thus, upon the first matrix crack,

$$\Delta\sigma_o = \frac{\sigma_c}{V_f} - E_f\varepsilon_c \tag{4}$$

where $\sigma_c$ = applied composite stress
$V_f$ = fiber volume fraction
$E_f$ = elastic modulus of fibers
$\varepsilon_c$ = composite strain
$\Delta\sigma_o$ = additional fiber stress after matrix crack at the crack tip

This gives the following expression for matrix stress along the fiber:

$$\sigma_m = \frac{V_f}{V_m}\Delta\sigma_o\left(1 - e^{-\phi^{1/2}x}\right) \tag{5}$$

where $$\phi^{1/2} = \frac{1}{r_f}\left\{\frac{-2(E_fV_f+E_m(1 - V_f))}{E_f(1 - V_f)(1 + \nu_m)\ln[(2\sqrt{3}/\pi)V_f]}\right\}^{1/2}$$

The distance, L, at which 95 percent load transfer occurs may be calculated from

$$L = -\phi^{-1/2}\ln\left(1 - \frac{\sigma_m(L)}{\sigma_m^{\infty}}\right) \tag{6}$$

where $$\frac{\sigma_m(L)}{\sigma_m^{\infty}} = \frac{\sigma_m(L)}{E_m \varepsilon_c} = 0.95$$

Note that because this case considers complete bonding, it is analogous to the Cox model in that the minimum crack spacing, 2L, is independent of applied load.

*McCartney Model*

McCartney [8] derived an elasticity model in 1989 as an attempt to improve upon the two models discussed earlier. The McCartney model uses some of the same basic ideas as the Cox and ACK models with a few major differences. The main difference is that this model is not a one-dimensional shear-lag model, rather it is an elasticity model that is able to account for three-dimensional stress effects. Another major difference is the inclusion of effects from thermal residual stresses that are induced in the composite during processing due to the mismatch of thermal expansion coefficients between the fiber and matrix. This forces the model to satisfy stress-strain-temperature relations as well as stress equilibrium and displacement compatibility conditions. In this model, two of four stress-strain-temperature relations are satisfied exactly, while the other two are satisfied in an average sense, as are the compatibility conditions. In order to satisfy the equilibrium and stress boundary conditions, all stress components that are relevant to the problem are retained, which is not the case in the other models used in this study. The McCartney model was programmed for the fully bonded case using the 95 percent load transfer criterion, and as with the other models, the crack spacing was independent of stress level.

## TEST RESULTS AND DISCUSSION

Neat Matrix Fatigue Tests

In the strain-controlled fatigue tests of the neat Timetal®21S matrix material for which the cyclic strain was well within the elastic region, the stress-strain hysteresis loop became stabilized within the first five to ten cycles (Figure 2). The hysteresis behavior remained stable until a dramatic load drop ensued just before final fracture. This was represented by plotting the elastic loading and unloading moduli (the slopes of the initial portions of the loading and unloading halves of the hysteresis loops) as a function of the number of applied cycles throughout a single test (Figure 3). The stiffness remained relatively constant for the entire test up to the point at which the large decrease in load began. In the tests performed at the upper two strain levels, some elastic-

plastic behavior occurred in the material. Because of this, the hysteresis loop took much longer to stabilize and the load drop before fracture was less dramatic than in the other tests.

The strain-life results obtained from these tests show a consistent behavior with a fairly low amount of scatter in fatigue life (Table 2). For the R = 0.1 strain ratio, the endurance limit was estimated to be $\Delta\varepsilon = 0.0045$. Compared with neat Ti-15-3 [9], the Timetal®21S has a greater fatigue resistance (Figure 4).

Unnotched Composite Fatigue Tests

*Stress-Strain Behavior*

The stress-strain behavior of the unnotched SCS-6/Timetal®21S $[0/90]_{2S}$ laminates showed a very distinct "knee" at approximately 150MPa of the first cycle (Figure 5). This bilinear first cycle loading response was similar to the results for the SCS-6/Ti-15-3 composite observed by Johnson et al. [1] who showed that this knee represents the point at which debonding of the fiber/matrix interface occurs in the transversely loaded plies of the composite. This interface debonding in the SCS-6/Timetal®21S was confirmed with edge replicas taken prior to loading the specimens and at the peak stress level of the first cycle. The unloading half of the first cycle does not exhibit the existence of such a knee, and a slight strain offset results upon reaching zero load. This suggests that permanent matrix damage occurred during the first cycle. The damage could be in the form of matrix cracking or local plasticity of the matrix material around the debonded transverse fibers.

For the second and several subsequent cycles, the overall stress-strain behavior followed the path of the unloading half of the first cycle (Figure 5). In these curves, the knee is still apparent under close observation, yet it is not as distinct as in the first cycle. Also, it is difficult to distinguish the exact stress level at which it occurs, however, it does appear to occur at a stress level slightly lower than the stress at the first cycle knee. Johnson et al. [1] have shown for SCS-6/Ti-15-3 that after the first cycle, the knee occurs when the applied stress in the transverse plies exceeds the thermal radial residual stress in the matrix. At stresses above the knee, the matrix is free to pull away from the fibers, resulting in a decrease of stiffness.

The initial loading modulus in cycles after the first cycle was also considerably lower than in the first cycle. This could be the result of the damage that occurred in the first cycle, since the stiffness will decrease due to either matrix cracking, 90 degree fiber/matrix separation, or the

existence of local matrix plasticity which would slightly relax the residual stresses that hold the matrix around the transverse fibers. This residual stress relaxation also explains the fact that the knee in the loading curve becomes less obvious after the first cycle. In fact, this knee is essentially negligible, and the loading curve may be approximated as a straight-line resulting in an average loading modulus This is observed for the second cycle shown in Figure 5.

The ratio of the average cyclic loading modulus to the initial first cycle loading modulus, $E_I$, represented in Figure 5 as a function of the number of applied cycles for a given test is shown in Figure 6. This shows, that after the original stiffness drop following the first cycle, the stiffness remained fairly constant until a steady drop occurred just prior to final fracture. This decrease in stiffness near the end of the test caused an increase in the maximum and minimum strain levels, as is shown in Figure 7. In addition, Figure 7 shows that the maximum strain increased at a higher rate than the minimum strain near the end of the test. This indicates that the loading curve shifted to the right along the strain axis in conjunction with a decrease in the slope.

*Stress-Life Behavior*

The unnotched fatigue behavior of the $[0/90]_{2S}$ laminates of the SCS-6/Timetal®21S composite showed fairly consistent results (Table 3). When comparing the results of the two different stress ratios on a maximum stress basis, the tests run at R = 0.3 had greater lives than those run at R = 0.1. This is to be expected, since for the same maximum stress, a stress ratio of R = 0.1 gives a greater stress range than does R = 0.3. If these results are compared on a stress range basis, the two fatigue curves collapse onto nearly the same curve, as is seen in Figure 8 [10]. Typically, for a stress range based comparison, longer fatigue lives are observed for lower stress ratios. Figure 8 shows a slight indication of that trend, however it is essentially negligible. This implies that there is no distinguishable stress ratio effect between R = 0.1 and R = 0.3.

The SCS-6/Timetal®21S and SCS-6/Ti-15-3 results were compared using a zero-degree-fiber stress range parameter. Johnson et al. [1] have shown that for the SCS-6/Ti-15-3 composite, the fatigue lives of several different lay-ups containing longitudinal plies could be represented with this parameter, collapsing the results onto one fatigue curve that describes the fatigue behavior of the composite. The zero-degree-fiber stress range, $\Delta\sigma_f^o$, is defined as

$$\Delta\sigma_f^o = E_f \Delta\varepsilon_c \qquad (7)$$

Because of the common fiber relationship between the Ti-15-3 and Timetal®21S matrix composites, one might expect that a comparison of this type would give very similar results. However, the fatigue lives of the SCS-6/Timetal®21S composite were shorter than those of the SCS-6/Ti-15-3 composite (Figure 9) [10]. This is in direct contrast with the neat matrix results, in which the Timetal®21S material had longer lives than the Ti-15-3 material. One potential reason for this is that the fiber strength between batches may vary. Other possible explanations may be that the fiber/matrix interface bond strengths of the two composites may be different, and that the Timetal®21S material could be more notch sensitive than Ti-15-3. This notch sensitivity is important, because the debonding of the fiber/matrix interface in the 90° plies causes an effective notch at stress levels above the knee in the stress-strain curve.

*Fatigue Cracking of Titanium Matrix*

At low stress levels, matrix fatigue cracking plays a very important role in the life of the composite material. Edge replicas taken under load revealed the existence of multiple matrix fatigue cracks emanating from the 90 degree ply fibers. This was observed late in the lives of specimens cycled at low stress levels (Figure 10). This behavior was also observed by Bakuckas et al. for SCS-6/Ti-15-3 [11]. The fatigue crack initiation occurred at this location due to the high matrix hoop strain acting around the debonded fibers in the loading direction. This matrix cracking was also observed when examining the final fracture surfaces with the scanning electron microscope. Multiple initiation sites were observed, as well as large areas of ductile fracture of the matrix material. Step fracture was also a common mode of fracture in these tests, implying that damage occurred at many sites on several different planes (Figure 11).

A phenomena that was observed for all tests lasting longer than approximately 30,000 cycles was the existence of evenly spaced surface cracks throughout the length of the specimens. In most cases, these cracks were first observed near the center of the test specimens and then grew out through the width toward the edges. This resulted in a series of matrix cracks which ran nearly the width of the specimens (Figure 12). The fact that this surface matrix cracking was only observed in longer life tests suggests that failure at high stress levels may be primarily fiber dominated. At lower stress levels, this matrix cracking would increase the composite strain, which in turn would raise the stress in the longitudinal fibers leading to failure of the composite. This is confirmed in Figure 7, which shows that the maximum and minimum composite strain levels for that particular test increased significantly between 20,000 and 30,000 cycles, corresponding to when extensive surface cracking was observed.

Comparison of Experimental Crack Spacing with Cylinder Models

It has been shown that the predictions of minimum length between two matrix cracks, 2L, is independent of the applied stress level for a fully bonded fiber/matrix interface. The minimum crack spacing predictions will vary based on the different exponential tendencies of the individual models. When comparing these models, the exponential tendency of the McCartney model is the strongest, resulting in the shortest crack spacing predictions, and that of the Cox model is the weakest, resulting in the longest crack spacing predictions.

For the group of tests in which evenly spaced matrix cracks existed along the specimen surface, the specimens with longer fatigue lives had higher crack densities, and hence shorter crack spacing. This was the case because as a given specimen was cycled, matrix cracks initiated between two existing cracks. This can occur, because although it would take an increase in load to generate further cracking in a static tensile test, multiple matrix cracks develop cumulatively at the same load under a fixed amplitude fatigue situation [5]. Because further testing at stress levels below those run in this study may result in a further increase in crack densities, it was impossible to obtain the minimum possible crack spacing for the SCS-6/Timetal®21S composite from this group of tests. However, it was assumed that for the test which was run for the greatest number of cycles, the cracks had become nearly saturated at the time of final specimen fracture. The minimum spacing for this test was found to be approximately 0.7 mm. The Cox, ACK, and McCartney models predicted minimum crack spacing values of 0.57, 0.36, and 0.32mm, respectively, compared to 0.66, 0.42, and 0.36mm for the SCS-6/Ti-15-3 composite. These values are lower than was observed.

## SUMMARY AND CONCLUSIONS

Fatigue tests have been performed on unnotched cross-ply laminates of SCS-6/Timetal®21S composite specimens. These specimens were tested at two different stress ratios in order to determine the effects of stress ratio on fatigue lives. Several strain-controlled fatigue tests were also run on the matrix material. Many of the results from these tests were compared to previous results obtained for the SCS-6/Ti-15-3 composite system. The following conclusions can be made from the results obtained in this study:

1. Strain-controlled fatigue tests on the Timetal®21S neat matrix material resulted in slightly longer fatigue lives than those published for the Ti-15-3 neat matrix.

2. Stress-controlled fatigue testing of unnotched $[0/90]_{2S}$ SCS-6/Timetal®21S composite specimens showed no difference in fatigue lives between stress ratios of R = 0.1 and R = 0.3 when compared on an applied stress range basis.

3. On a zero-degree-fiber stress range basis, the SCS-6/Timetal®21S composite system had lower fatigue lives than did the SCS-6/Ti-15-3 composite system. This is in contrast with the fatigue results of the neat matrix materials. Variable fiber properties and possible differences in fiber/matrix interface strengths between the two systems are potential causes for this discrepancy.

4. Examination of fracture surfaces of the unnotched composite specimens revealed multiple crack initiation sites and areas of step fracture. This implies that fracture was not caused from one major crack front. Edge replicas also showed many internal cracks emanating from the transverse fibers. This may be due to local stress concentrations at the fibers after separation of the fiber/matrix interface. In addition, all fatigue tests which lasted longer than approximately 30,000 cycles had visible matrix cracks on the outer surface that were evenly spaced throughout the length of the specimens. This matrix cracking considerably reduced the elastic modulus of the composite, resulting in greater strains leading to final fracture of the specimens.

## ACKNOWLEDGMENT

The work and materials used in this study were funded by NASA Langley Research Center through GWP 85B, and directed by Dr. W. S. Johnson.

## REFERENCES


[1] Johnson, W. S., Lubowinski S. J, and Highsmith, A. L., "Mechanical Characterization of Unnotched SCS-6/Ti-15-3 Metal Matrix Composites at Room Temperature," Thermal and Mechanical Behavior of Ceramic and Metal Matrix Composites, ASTM STP 1080, Kennedy, Moulller, and Johnson, Eds., American Society for Testing and Materials, 1990, pp. 193-218.

[2] McKeighan, P. C., Evans, R. D., and Hillberry, B. M., "Fatigue and Fracture Testing Using a Multitasking Minicomputer Workstation," Applications of Automation Technology to Fatigue and Fracture Testing, ASTM STP 1092, A. A. Braun, N. E. Ashbaugh, and F. M. Smith Eds., American Society for Testing and Materials, Philadelphia, 1990, pp. 52-67.

[3] Cox, H. L., "The Elasticity and Strength of Paper and Other Fibrous Materials," British Journal of Applied Physics, Vol. 3, March 1952, pp. 72-79.

[4] Kelly, A. and Macmillan, N. H., Strong Solids, 3rd Edition, Oxford: Clarendon Press, 1986.

[5] Hillberry, B. M. and Johnson, W. S., "Fatigue Crack Spacing in the Matrix of a Continuous Fiber SCS-6/Ti Composite," To be Published, Journal of Composites Technology and Research, Vol. 15, No.3, Fall 1993.

[6] Aveston, J. and Kelly, A., "Theory of Multiple Fracture of Fibrous Composites," Journal of Materials Science, Vol. 8, 1973, pp. 352-362.

[7] Aveston, J., Cooper, G. A., and Kelly, A., "The Properties of Fibre Composites," Conference Proceedings, National Physical Laboratory, IPC Science and Technology Press Ltd, 1971, p. 15.

[8] McCartney, L. N., "New Theoretical Model of Stress Transfer Between Fibre and Matrix in a Uniaxially Fibre-Reinforced Composite," Proc. R. Soc. Lond., A 425, 1989, pp. 215-244.

[9] Hillberry, B. M. and Johnson, W. S., "Prediction of Matrix Fatigue Crack Initiation in Notched SCS-6/Ti-15-3, Metal Matrix Composites," NASA TM-104141, National Aeronautics and Space Administration, Washington, D. C., Oct. 1991, 14 pp.

[10] Ward, G. T., Herrmann, D. J., and Hillberry, B. M., "Stress-Life Behavior of Unnotched SCS-6/Ti-β21S Cross-Ply Metal Matrix Composites at Room Temperature," Fatigue 93 Proceedings, Eds. J.-P. Bailon and J. I. Dickson, pp. 1067-1072.

[11] Bakuckas, J. G., Jr., Johnson, W. S., and Bigelow, C. A., "Fatigue Damage in Cross-Ply Titanium Metal Matrix Composites Containing Center Holes," NASA TM-104197, National Aeronautics and Space Administration, Washington, D. C., January, 1992, 29 pp.

[12] Mirdamadi, M. and Johnson, W. S., "Stress-Strain Analysis of a $[0/90]_{2S}$ Titanium Matrix Laminate Subjected to a Generic Hypersonic Flight Profile," NASA TM-107584, National Aeronautics and Space Administration, Washington, D. C., March 1992, 25 pp.

Table 1. Mechanical properties of fiber and matrix.

| Property | Fiber (SCS-6) | Matrix (Timetal®21S) |
|---|---|---|
| Young's Modulus, E (GPa) | 400 | 112 [1] |
| Yield Strength, $S_y$ (MPa) | | 1050 [2] |
| Ultimate Strength, $S_u$ (MPa) | 3450 | 1150 [2] |
| Poisson Ratio, $\nu$ | 0.25 | 0.35 |
| C.T.E., $\alpha$ (mm/mm/°C) [3] | $3.794 \times 10^{-6}$ [12] | $9.476 \times 10^{-6}$ [4] |

1) Measured for this study
2) Data from Noel Ashbaugh, University of Dayton Research Institute
3) Average C.T.E.'s for $\Delta T$ from 621.1°C to 21.1°C
4) Data from Massoud Mirdamadi, NASA Langley Research Center

Table 2. Fatigue data from strain-controlled fatigue tests of the neat Timetal®21S matrix material.

| $\varepsilon_{max}$ [mm/mm] | $\Delta\varepsilon$ [mm/mm] | $\sigma_{max}$ [MPa] | $\Delta\sigma$ [MPa] | Cycles to Failure, N |
|---|---|---|---|---|
| 0.00939 | 0.00852 | 983 | 977 | 6,760 |
| 0.00895 | 0.00805 | 983 | 926 | 7,848 |
| 0.00801 | 0.00720 | 855 | 755 | 13,680 |
| 0.00750 | 0.00680 | 851 | 769 | 15,724 |
| 0.00721 | 0.00648 | 785 | 681 | 18,345 |
| 0.00674 | 0.00609 | 761 | 686 | 18,949 |
| 0.00641 | 0.00576 | 701 | 604 | 30,164 |
| 0.00594 | 0.00536 | 678 | 605 | 32,794 |
| 0.00559 | 0.00503 | 636 | 562 | 40,521 |
| 0.00517 | 0.00466 | 583 | 523 | 65,000 |
| 0.00513 | 0.00460 | 589 | 519 | 217,930 |
| 0.00504 | 0.00457 | 568 | 509 | >1,000,000* |
| 0.00475 | 0.00428 | 539 | 478 | >1,000,000* |

*Run-out

Table 3. Fatigue data from stress-controlled fatigue tests of unnotched SCS-6/Timetal®21S $[0/90]_{2S}$ cross-ply laminates.

| Fiber Volume Fraction, $V_f$ | $\sigma_{max}$ [MPa] | $\Delta\sigma$ [MPa] | $\varepsilon_{max}$ [mm/mm] | $\Delta\varepsilon$ [mm/mm] | Cycles to Failure, N |
|---|---|---|---|---|---|
| 0.365 | 768 | 688 | 0.00590 | 0.00519 | 3,163 |
| 0.365 | 736 | 666 | 0.00563 | 0.00494 | 4,355 |
| 0.365 | 686 | 621 | 0.00529 | 0.00462 | 9,795 |
| 0.365 | 636 | 571 | 0.00480 | 0.00427 | 11,555 |
| 0.365 | 567 | 509 | 0.00424 | 0.00379 | 14,190 |
| 0.365 | 498 | 450 | 0.00371 | 0.00338 | 18,612 |
| 0.365 | 469 | 424 | 0.00341 | 0.00302 | 35,012 |
| 0.365 | 423 | 384 | 0.00301 | 0.00275 | 56,432 |
| 0.365 | 325 | 292 | 0.00232 | 0.00206 | 367,300 |
| 0.354 | 815 | 574 | 0.00654 | 0.00441 | 9,161 |
| 0.354 | 764 | 537 | 0.00631 | 0.00420 | 8,564 |
| 0.354 | 693 | 487 | 0.00530 | 0.00362 | 15,190 |
| 0.354 | 583 | 410 | 0.00489 | 0.00328 | 29,547 |
| 0.354 | 507 | 356 | 0.00398 | 0.00294 | 60,597 |
| 0.354 | 448 | 315 | 0.00344 | 0.00240 | 94,796 |

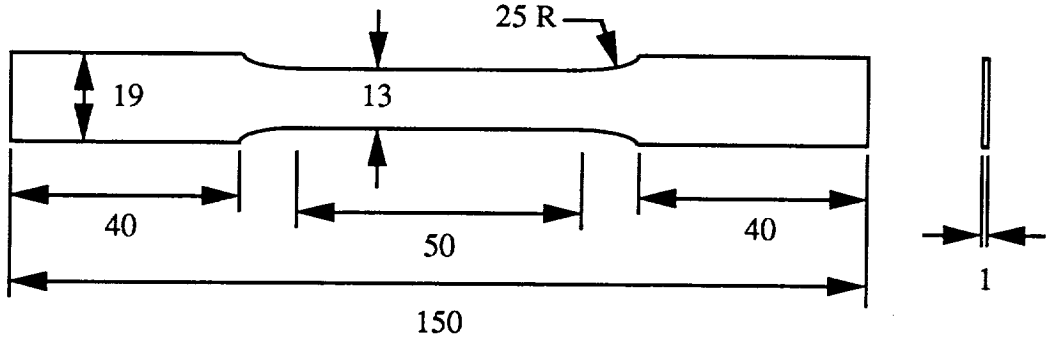


(a)

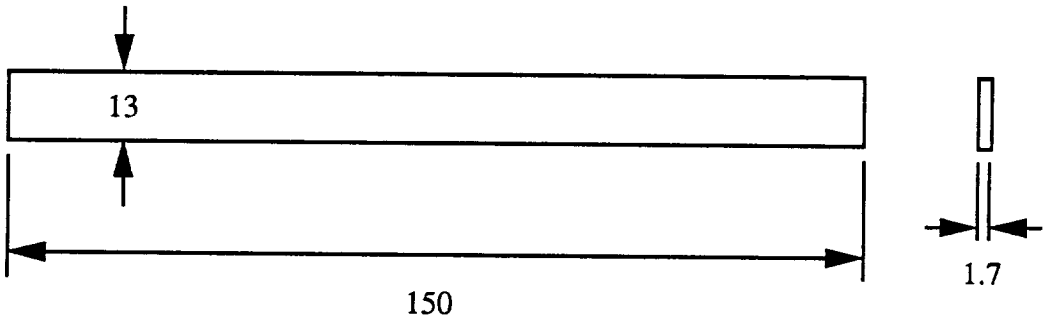


(b)

Figure 1. Geometries of test specimens used in this research.
(a) neat matrix dogbone specimen, (b) composite unnotched specimen.
All dimensions shown in mm.

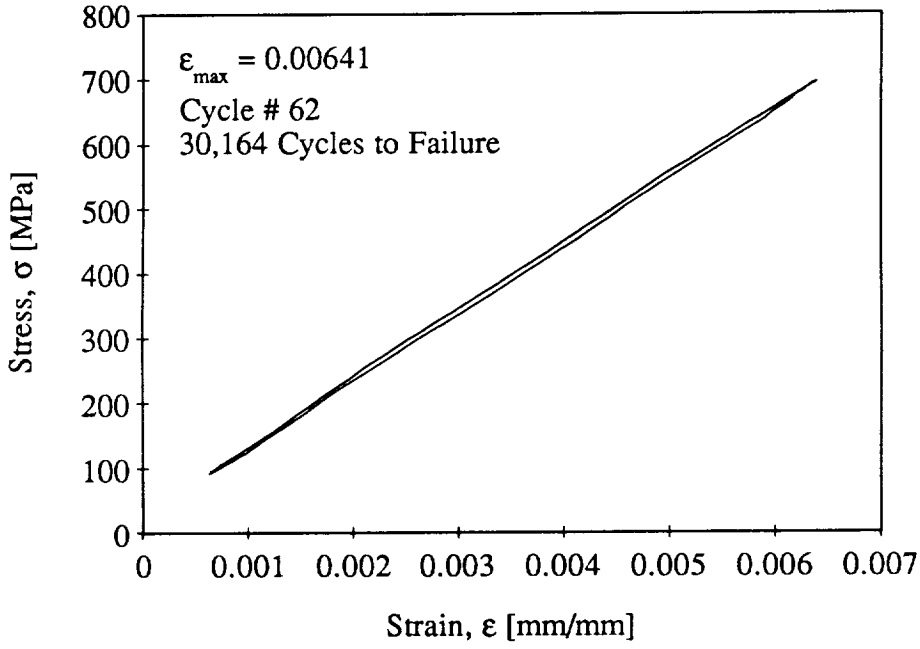


Figure 2. Typical stabilized hysteresis loop for Timetal®21S. R = 0.1.

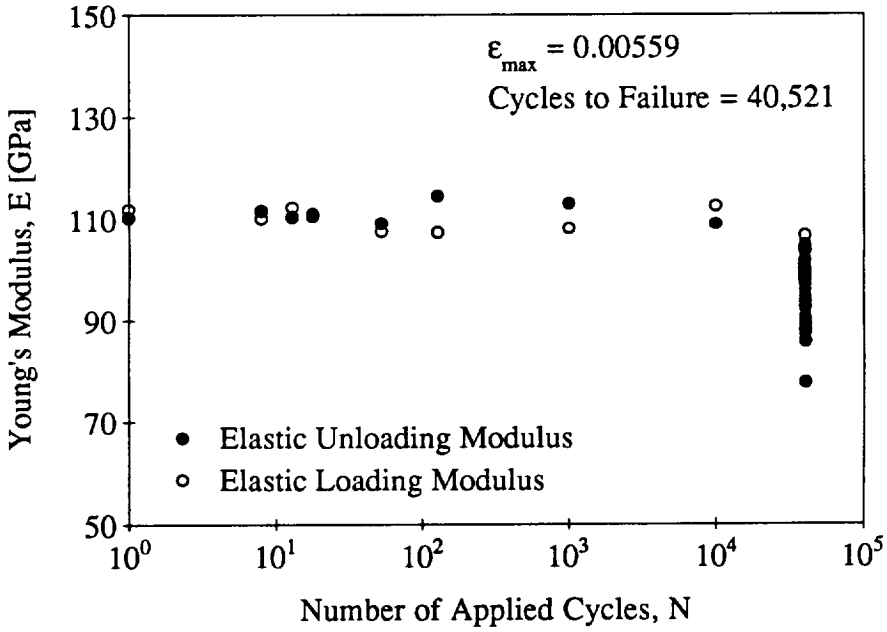


Figure 3. Loading and unloading elastic moduli versus number of applied cycles for a given fatigue test of Timetal®21S. R = 0.1.

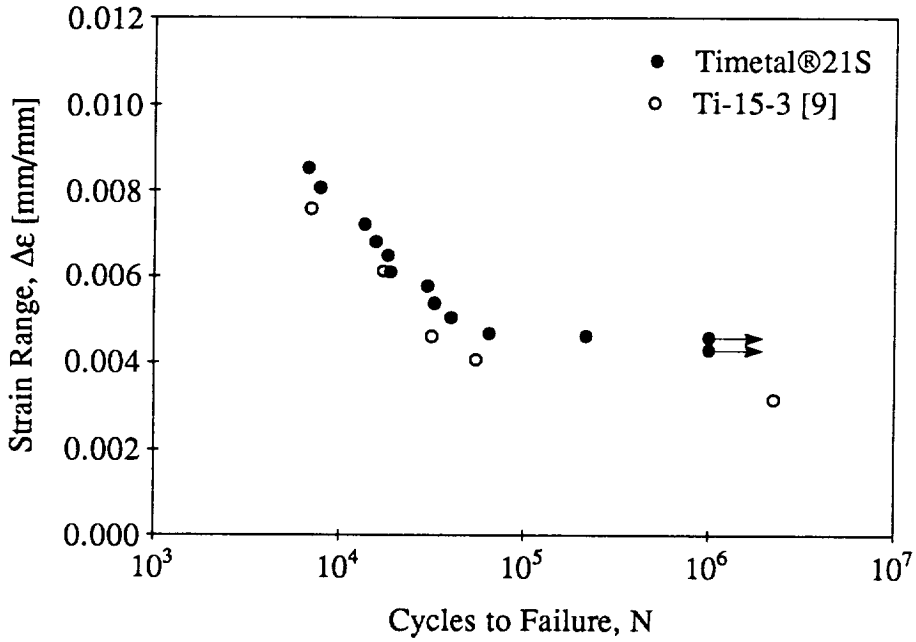


Figure 4. Comparison of fatigue lives between the Timetal®21S and Ti-15-3 neat matrix materials as a function of the strain range. R = 0.1.

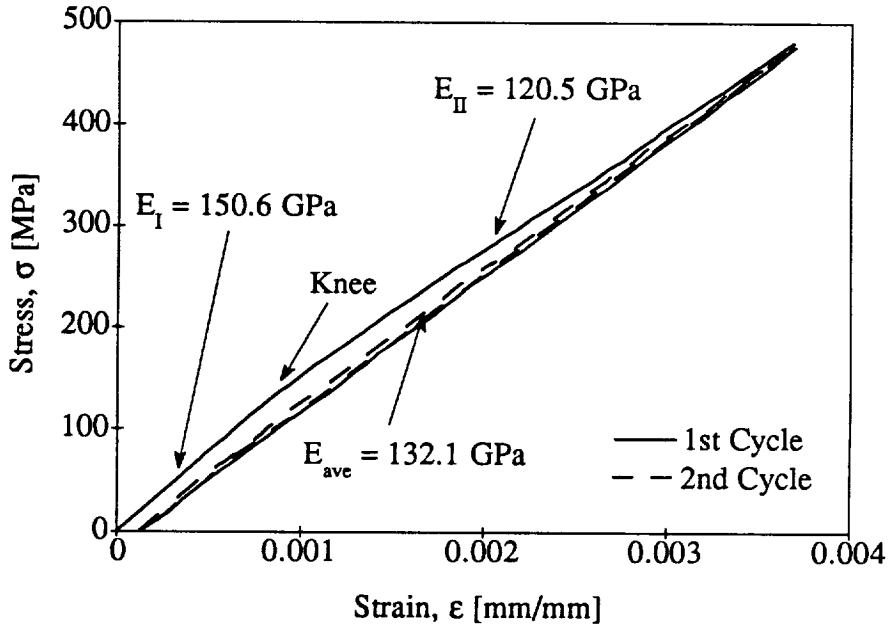


Figure 5. Comparison of the stress-strain response of the first and second fatigue cycles for the SCS-6/Timetal®21S composite.

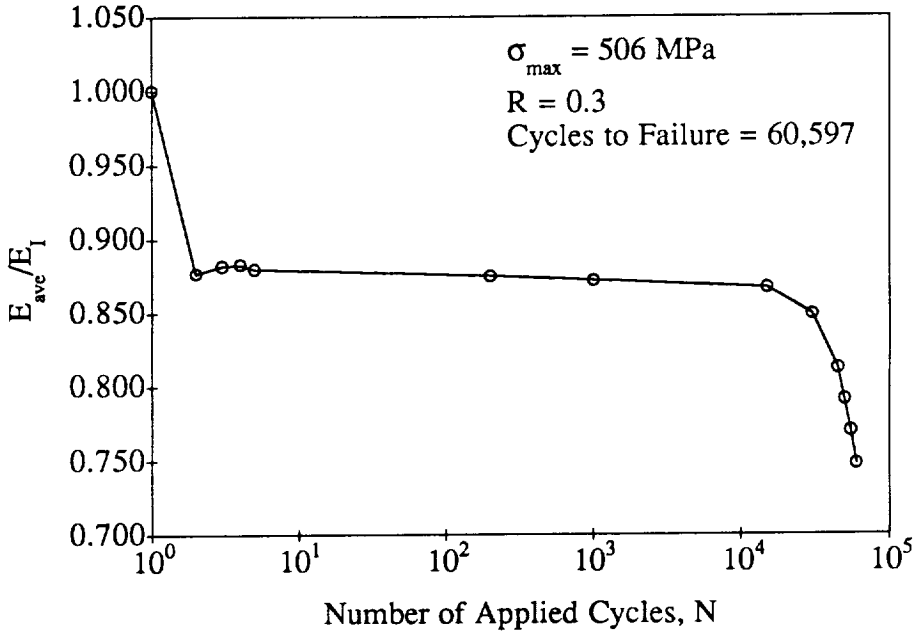


Figure 6. Ratio of average loading modulus to initial first cycle loading modulus versus the number of applied cycles for a given fatigue test of SCS-6/Timetal®21S.

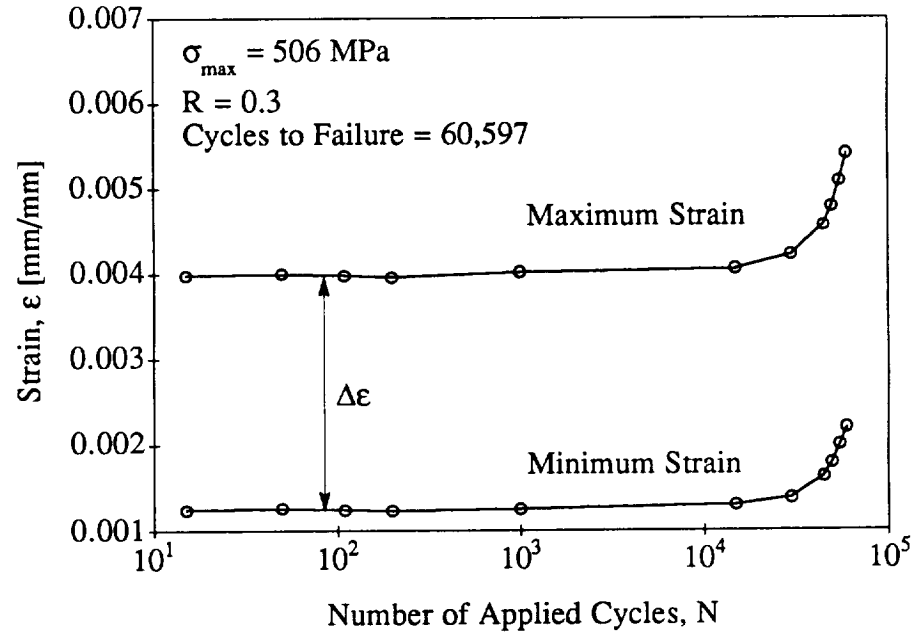


Figure 7. Maximum and minimum strain versus the number of applied cycles for the fatigue test shown in Figure 6.

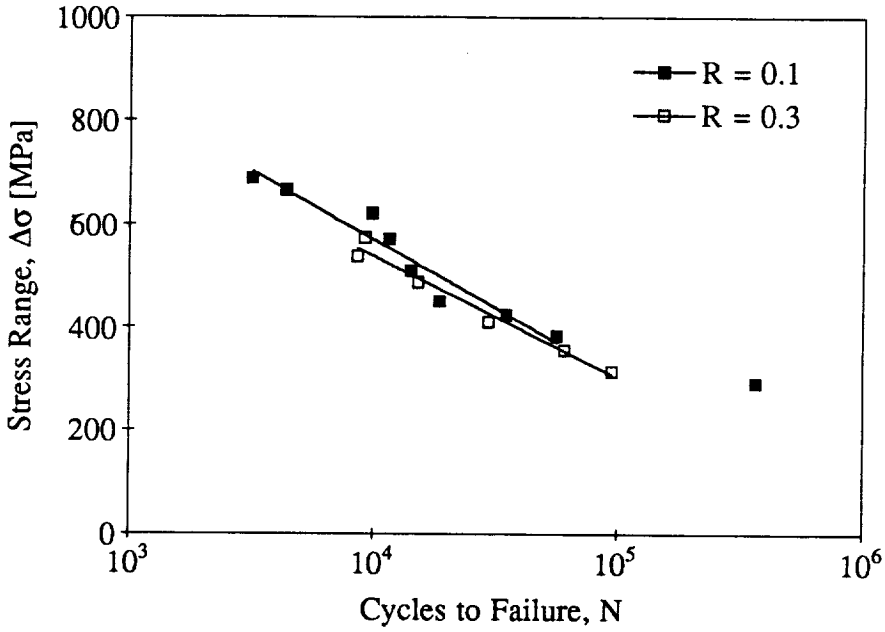


Figure 8. Stress range versus life curve for unnotched SCS-6/Timetal®21S $[0/90]_{2S}$ composites at R = 0.1 and R = 0.3 [10].

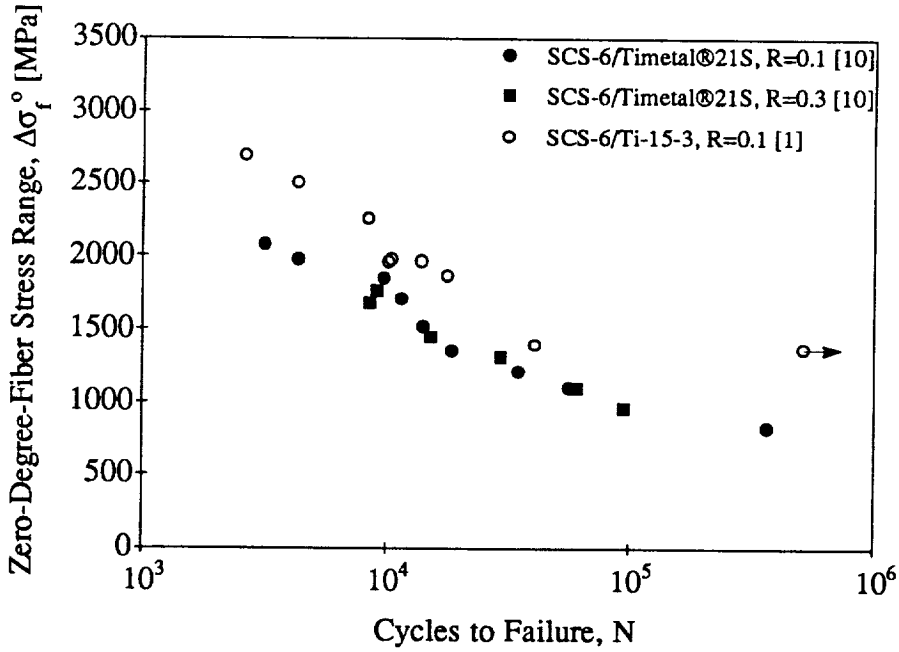


Figure 9. Comparison of fatigue lives between the SCS-6/Timetal®21S and SCS-6/Ti-15-3 unnotched composites as a function of the zero-degree-fiber stress range.

$\sigma_{max}$ = 469 MPa

R = 0.1

Cycles = 35,000

Mag. = 200X

Edge Replica at $\sigma_{mean}$ = 256 MPa

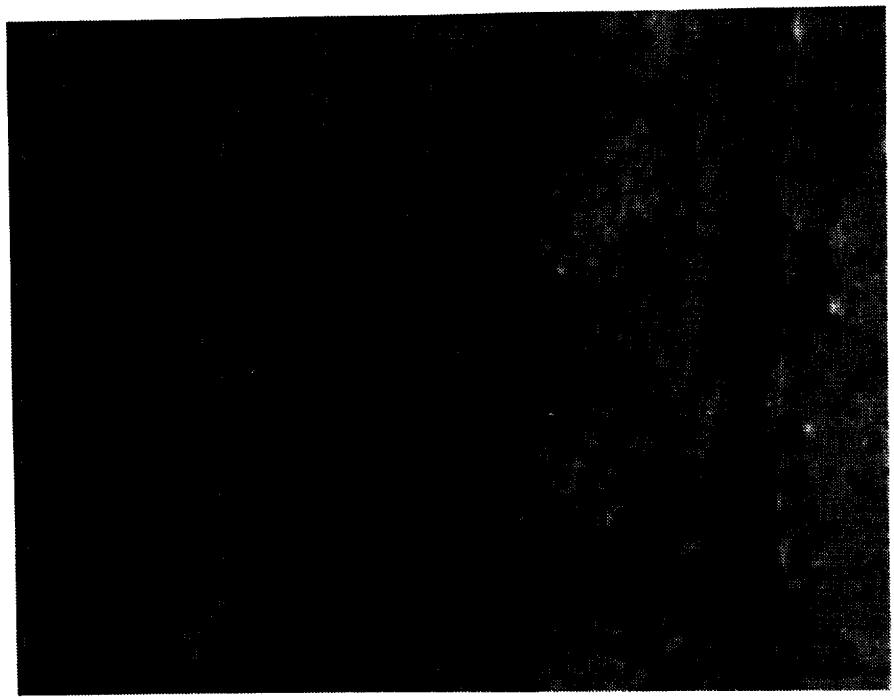

Figure 10. Edge replica taken under load of an SCS-6/Timetal®21S $[0/90]_{2S}$ composite specimen showing multiple matrix cracks from 90° fibers.

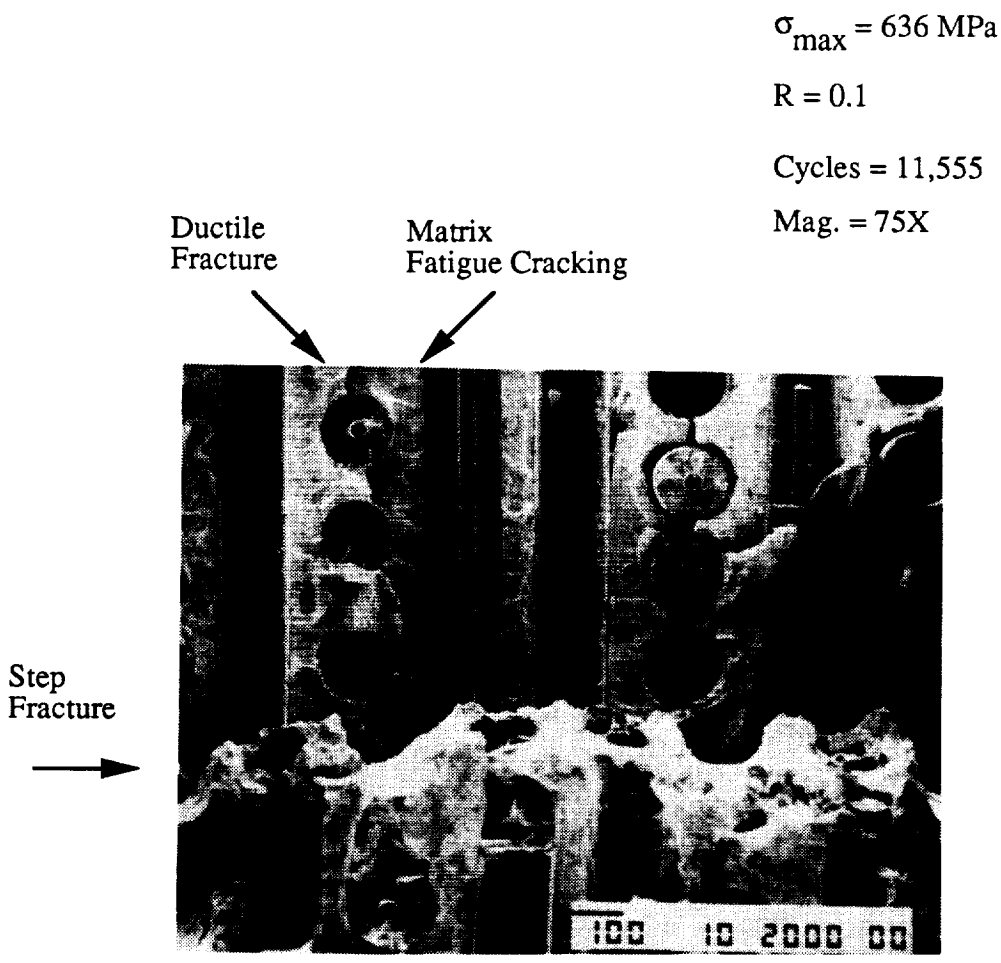


Figure 11. SEM fractograph of SCS-6/Timetal®21S $[0/90]_{2S}$ composite showing regions of fatigue crack growth and ductile rupture, as well as step fracture. Loading was perpendicular to page.

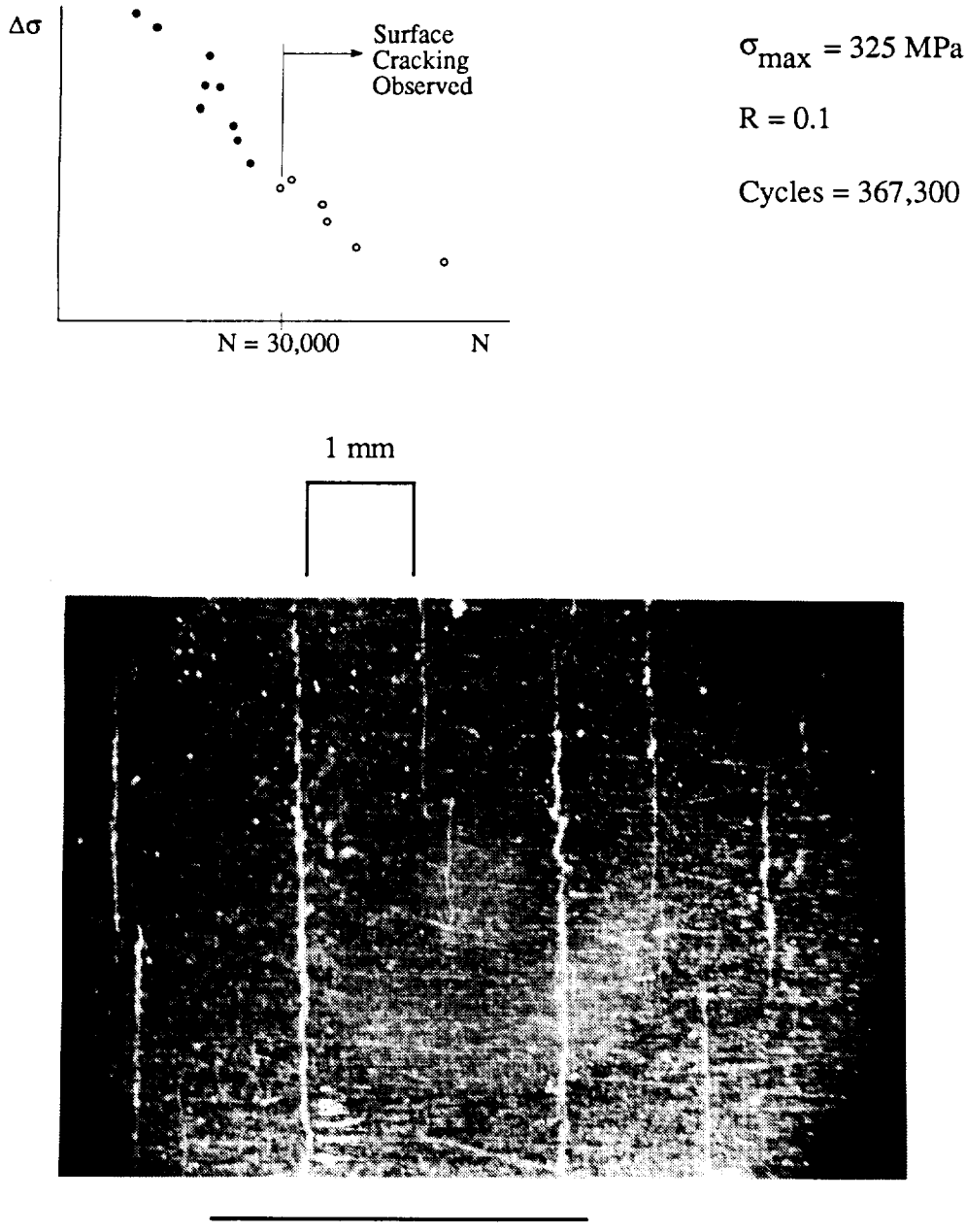


Figure 12. Photograph showing multiple surface cracking along length of unnotched SCS-6/Timetal®21S $[0/90]_{2S}$ composites.

# REPORT DOCUMENTATION PAGE

Form Approved
OMB No. 0704-0188



| 1. AGENCY USE ONLY (Leave blank) | 2. REPORT DATE | 3. REPORT TYPE AND DATES COVERED |
|---|---|---|
| | July 1993 | Contractor Report |

**4. TITLE AND SUBTITLE**

Fatigue-Life Behavior and Matrix Fatigue Crack Spacing in Unnotched SCS-6/Timetal®21S Metal Matrix Composites

**5. FUNDING NUMBERS**

NAG1-1316
WU 763-23-45-85

**6. AUTHOR(S)**

G. T. Ward, D. J. Herrmann, and B. M. Hillberry

**7. PERFORMING ORGANIZATION NAME(S) AND ADDRESS(ES)**

Purdue University
School of Mechanical Engineering
West Lafayette, IN 47907-1288

**8. PERFORMING ORGANIZATION REPORT NUMBER**

**9. SPONSORING/MONITORING AGENCY NAME(S) AND ADDRESS(ES)**

National Aeronautics and Space Administration
Langley Research Center
Hampton, VA 23681-0001

**10. SPONSORING/MONITORING AGENCY REPORT NUMBER**

NASA CR-191467

**11. SUPPLEMENTARY NOTES**

Langley Technical Monitor: W. Steven Johnson
Final Report

**12a. DISTRIBUTION/AVAILABILITY STATEMENT**

Unclassified - Unlimited

Subject Category - 39

**12b. DISTRIBUTION CODE**

**13. ABSTRACT** *(Maximum 200 words)*

Fatigue tests of the SCS-6/Timetal®21S composite system were performed to characterize the fatigue behavior for unnotched conditions. The stress-life behavior of the unnotched $[0/90]_{2S}$ laminates was investigated for stress ratios of R = 0.1 and R = 0.3. The occurrence of matrix cracking was also examined in these specimens. This revealed multiple matrix crack initiation sites throughout the composite, as well as evenly spaced surface cracks along the length of the specimens. No difference in fatigue lives were observed for stress ratios of R = 0.1 and R = 0.3 when compared on a stress range basis. The unnotched SCS-6/Timetal®21S composites had shorter fatigue lives than the SCS-6/Ti-15-3 composites, however the neat Timetal®21S matrix material had a longer fatigue life than the neat Ti-15-3.

**14. SUBJECT TERMS**

Fatigue; Titanium matrix; Silicon-carbide fibers; Unnotched; Cross-ply laminates; Matrix fatigue crack spacing

**15. NUMBER OF PAGES**

26

**16. PRICE CODE**

A03

| 17. SECURITY CLASSIFICATION OF REPORT | 18. SECURITY CLASSIFICATION OF THIS PAGE | 19. SECURITY CLASSIFICATION OF ABSTRACT | 20. LIMITATION OF ABSTRACT |
|---|---|---|---|
| Unclassified | Unclassified | | |